

Percolation Effects on Adsorption–Desorption Hysteresis

R. H. López,* A. M. Vidales, and G. Zgrablich

Laboratorio de Ciencias de Superficies y Medios Porosos, Universidad Nacional de San Luis,
Chacabuco 917, 5700 San Luis, Argentina

Received November 9, 1999. In Final Form: May 22, 2000

In the present work we study how the adsorption–desorption hysteresis loop of a mesoporous-disordered medium represented by a three-dimensional dual site-bond model is affected by percolation for different kinds of site and bond distributions. The behavior of the threshold pressure for the evaporation process, as a function of the separation between the site and bond distributions and their dispersions, suggests a method to determine them from experimental adsorption–desorption hysteresis curves.

1. Introduction

The problem of the characterization of porous media, i.e., the determination of their morphological properties from experimental data, involve both theoretical and experimental methods, which have extensively been reviewed in ref 1. Some of the experimental methods, like NMR, small-angle X-ray spectroscopy (SAXS), and small-angle neutron scattering (SANS), require sophisticated instruments while others, like porosimetry and adsorption–desorption of vapors, use much simpler apparatus, which can be available to practically any laboratory. Theoretical methods based on any of these experimental techniques require assuming a given geometrical shape for the pores, and this is an important general limitation. Adsorption–desorption of vapors, relying on the Kelvin condensation–evaporation process in a curved liquid–vapor interface, is particularly useful for mesoporous solids (pore sizes in the range 20–500 Å) used in a number of practical applications, especially catalysis.

From the above we see that the characterization of mesoporous materials, and in particular the determination of the pore size distribution, from adsorption–desorption experiments is a subject of great practical importance. However, as we shall see, this still stands as an open problem presenting interesting theoretical challenges,^{1–8} and this is more remarkable in the case of disordered (or amorphous) porous media. In fact, the shape and extent of the adsorption–desorption hysteresis loop (ADHL) of vapors in mesoporous materials are known to be influenced by several characteristics of the porous space; the geometrical shape of the pores, their size distribution, and the interconnectivity of the porous network are among those which have been studied intensively for a long time.

The problem has two aspects: In the first place, a model describing the properties of the medium must be given,

and then, within that model, a procedure to determine the pore size distribution must be developed. Modeling of porous media has evolved along two different, but complementary, lines: continuum and discrete models. Continuum models, based on a continuous characteristic function attaining the value 0 at an empty point and 1 at a solid point, have proven to be more adequate to study the flux of fluids through the medium.^{9–13} On the other hand, discrete models, representing the porous space by a network of voids (sites) connected by throats (bonds), have demonstrated to be a powerful tool to study the percolation properties of the medium and those phenomena depending on its topological properties.^{3,5,6,8,14–21}

Among the family of discrete models, the dual site–bond model (DSBM), introduced by Mayagoitia et al.³ is the simplest model which takes into account spatial correlation among pore sizes, allowing in this way to generate porous networks with different structures. Within the framework of this model, through analytical calculations on a Cayley tree (where no closed loops are involved)¹⁴ and through Monte Carlo simulations in two-dimensional networks,¹⁵ it has been shown that spatial correlation among pore sizes drastically affects percolation probabilities. It is then to be expected that in more realistic three-dimensional networks spatial correlation will have similar effects on the percolation probabilities and these, in turn, will affect the ADHL. Accordingly, the first, and central, purpose of this work is to study how the ADHL is influenced by spatial correlation as described by the DSBM. We remark that real disordered mesoporous

(1) Sahimi, M. *Flow and Transport in Porous Media and Fractured Rock*; VCH: Weinheim, 1995.

(2) Gregg, S. J.; Sing, K. S. W. *Adsorption, Surface Area and Porosity*; Academic Press: New York, 1982.

(3) Mayagoitia, V.; Gilot, B.; Rojas, F.; Kornhauser, I. *J. Chem. Soc., Faraday Trans.* **1988**, *1*, 84, 801.

(4) Mayagoitia, V. In *Characterization of Porous Solids III*; Rodriguez-Reinoso, F., Rouquerol, J., Sing, K. S., Unger, K. K., Eds.; Elsevier: Amsterdam, 1991; p 51.

(5) Seaton, N. A. *Chem. Eng. Sci.* **1991**, *46*, 1895.

(6) Zhdanov, V. P. *Adv. Catal.* **1993**, *39*, 1.

(7) Lastoskie, C. M.; Quirk, N.; Gubbins, K. E. In *Equilibria and Dynamics of Gas Adsorption on Heterogeneous Solid Surfaces*; Rudzinski, W., Steele, W. A., Zgrablich, G., Eds.; Elsevier: Amsterdam, 1997; p 745.

(8) Kornhauser, I.; Faccio, R. J.; Riccardo, J. L.; Rojas, F.; Vidales, A. M.; Zgrablich, G. *Fractals* **1997**, *5*, 355.

(9) Chaouche, M.; Rakotomala, N.; Salin, D.; Xu, B.; Yortsos, Y. C. *Chem. Eng. Sci.* **1994**, *49*, 2447.

(10) Sallés, J.; Thovert, J. F.; Adler, P. M. In *Characterization of Porous Solids III*; Rouquerol, J., Rodriguez-Reinoso, F., Sing, K. S. W., Unger, K. K., Eds.; Elsevier: Amsterdam, 1994.

(11) Giona, M.; Adrover, A. *AIChE J.* **1996**, *42*, 1407.

(12) Roberts, A. P.; Knackstedt, M. A. *Phys. Rev. E* **1996**, *54*, 2331.

(13) Loggia, D.; Salin, D.; Yortsos, Y. C. *Phys. Fluids* **1998**, *10*, 747.

(14) Faccio, R. J.; Zgrablich, G.; Mayagoitia, V. *J. Phys. C: Condens. Matter* **1993**, *5*, 1823.

(15) Vidales, A. M.; Faccio, R. J.; Riccardo, J. L.; Miranda, E. N.; Zgrablich, G. *Physica A* **1995**, *218*, 19.

(16) Vidales, A. M.; Faccio, R. J.; Zgrablich, G. *Langmuir* **1995**, *11*, 1178.

(17) Vidales, A. M.; Miranda, E.; Mayagoitia, V.; Rojas, F.; Zgrablich, G. *Europhys. Lett.* **1996**, *36*, 259.

(18) Vidales, A. M.; Miranda, E.; Rosen, M.; Zgrablich, G. In *Fractals and Chaos in Chemical Engineering*; Giona, M., Biardi, G., Eds.; World Scientific: Singapore, 1997.

(19) Xu, B.; Yortsos, Y. C.; Salin, D. *Phys. Rev. E* **1998**, *57*, 739.

(20) Vidales, A. M.; Miranda, E.; Zgrablich, G. *Int. J. Mod. Phys.* **1998**, *9*, 827.

(21) Vidales, A. M.; López, R.; Zgrablich, G. *Langmuir* **1999**, *15*, 5703.

materials are hardly conceivable as completely random media and that the determination of percolation probabilities in three-dimensional correlated porous networks is a nonsolved problem. Thus, our idea is to study directly the effects of spatial correlations on ADHL with the hope of finding a general empirical behavior.

The problem of obtaining the site and bond size distributions from the analysis of ADHL has been solved so far only for noncorrelated porous networks and in the extreme cases where the pore volume can be attributed either entirely to the sites or entirely to the bonds.^{6,22,23} It seems that the hypothesis that the main pore volume resides in the sites, while the bonds only play a role in the interconnectivity effects, is reasonable for a variety of porous solids,⁶ and to keep the present study simple with respect to all aspects which are relevant to our central purpose, such a hypothesis will be assumed in what follows. Our second purpose in this work is to take a first step toward the development of a method to determine the site and bond size distributions from the analysis of ADHL, for the general case of correlated porous networks.

The organization of the present work is as follows. In section 2 we briefly review the highlights of the DSBM. In section 3 we present a model to simulate the adsorption and desorption processes in three-dimensional correlated porous networks and to obtain ADHL. Results for ADHL corresponding to site-bond lattices with Gaussian and Gamma size distributions and for different correlation degrees are presented and discussed in section 4. In section 5 we test classical characterization methods (not considering spatial correlations) against simulation results, showing their limitations, and then we propose a method to obtain site and bond size distributions from experimental data on the basis of a quasi-universal empirical equation emerging from the analysis of all the above results. Finally, conclusions are given in section 6.

2. Dual Site–Bond Model (DSBM)

Let $S(R)$ and $B(R)$ be the distribution functions associated with the site and bond size R and $F_S(R)$ and $F_B(R)$ the corresponding probability density functions, such that

$$\begin{aligned} S(R) &= \int_0^R F_S(\mathcal{R}) d\mathcal{R} \\ B(R) &= \int_0^R F_B(\mathcal{R}) d\mathcal{R} \end{aligned} \quad (1)$$

and let the intervals $s = [s_1, s_2]$ and $b = [b_1, b_2]$ be the support of site and bond measures, i.e., the set of values of R for which F_S and F_B are positively defined. The way in which sites and bonds are connected to form the network is given by the joint probability density function, $F(R_S, R_B)$, of finding a site with size $R_S \in (R_S, R_S + dR_S)$ connected to a bond with size $R_B \in (R_B, R_B + dR_B)$. The two basic laws describing the DSBM are:

$$B(R) - S(R) \geq 0 \quad (2)$$

$$F(R_S, R_B) = 0 \quad \text{for } R_S < R_B \quad (3)$$

The first law, eq 2, implies that $b_1 \leq s_1$ and $b_2 \leq s_2$, while the second law, eq 3, called the *construction principle* (CP), is of a local nature and expresses the fact that the size R_B of any bond cannot be bigger than that of the two connected sites (in a porous medium the size of a throat cannot be larger than that of the two connected voids).

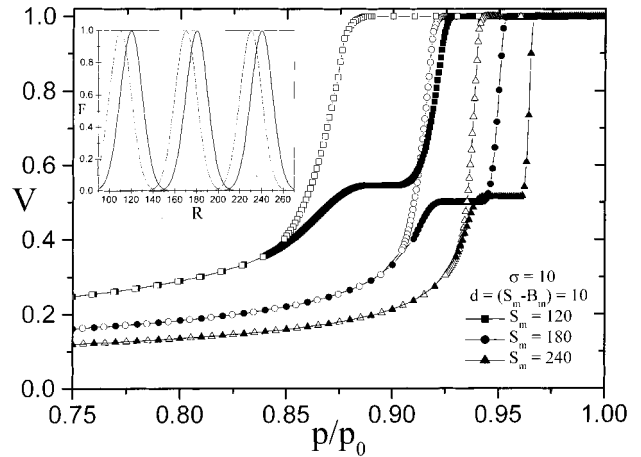


Figure 1. ADHL for Gaussian site and bond distributions for fixed σ and d showing the effect of the position of the site distribution. In the inset the site (thick line) and bond (thin line) distributions are represented for each case. Filled black symbols are used for the adsorption process and open ones for the desorption process.

If the joint probability function is expressed as

$$F(R_S, R_B) = F_S(R_S)F_B(R_B)\Phi(R_S, R_B) \quad (4)$$

then the correlation function Φ carries the information about the site-bond assignment procedure in the network. In the simplest case where sites and bonds are assigned to each other in the most random way as allowed by the CP, called the *self-consistent* case, then $\Phi(R_S, R_B)$ attains the following expression:

$$\Phi(R_S, R_B) = \frac{\exp\left[-\int_{R_B}^{R_S} \frac{dB}{B-S}\right]}{B(R_B) - S(R_B)} \quad (5)$$

If we denote by Ω the overlapping area between the site and bond probability density functions, as shown in Figure 1 for the simple case of uniform distributions, the function Φ has the following properties: (i) $\Phi_{\Omega=0}(R_S, R_B) = 1$, $\forall R_S, R_B$, sites and bonds are distributed completely at random, and (ii) $\Phi_{\Omega=0}(R_S, R_B) \propto \delta(R_S - R_B)$, $\forall R_S, R_B$, sites and bonds group together in macroscopic patches, each having a value of R . Then, the overlapping Ω is the fundamental parameter describing the topology of the network in this model.

This behavior also suggests that Ω must be related to some *correlation length* (which would be a physically more meaningful parameter), characteristic of the decay of the spatial correlation function defined as:

$$C(r) = \langle R_S(\vec{r}_0)R_S(\vec{r}_0 + \vec{r}) \rangle = \langle R_B(\vec{r}_0)R_B(\vec{r}_0 + \vec{r}) \rangle \quad (6)$$

In fact, it is expected that $C(r)$ decays approximately in an exponential form (this would be the exact behavior for a one-dimensional network generated by a Markov chain of events)

$$C(r) \approx \exp(-r/l_0) \quad (7)$$

where l_0 is the correlation length (measured in lattice constants). This expression has been used extensively in applications of the DSBM⁸ together with the ansatz

$$l_0 \approx \Omega/(1 - \Omega) \quad (8)$$

(22) Mason, G. *Proc. R. Soc. London, Ser. A* **1988**, 415, 453.

(23) Palar, M.; Yortsos, Y. C. *J. Colloid Interface Sci.* **1989**, 132, 425.

relating the overlapping with the correlation length, in such a way that $l_0 \rightarrow 0$ for $\Omega \rightarrow 0$ and $l_0 \rightarrow \infty$ for $\Omega \rightarrow 1$.

The problem of the generation of DSBM networks has been intensively investigated.^{3,8,24–28} We employ here the method presented in refs 8 and 25 for the Monte Carlo generation of such networks, which can be resumed in the following very simple terms. An initial network is prepared by sampling the values of R_S and R_B from the corresponding probability density functions F_S and F_B and distributing them completely at random on the lattice. This network will have the correct F_S and F_B but not the correct $\Phi(R_S, R_B)$; in particular the CP is not obeyed everywhere. Then a Markov chain of new states of the network is generated by choosing at random pairs of sites (or bonds) and attempting to exchange them; the exchange is accepted if it does not violate the CP. It has been demonstrated²⁵ that this procedure leads finally to the equilibrium distribution for the network and that it does not suffer the imperfections introduced by other methods (mainly anisotropy).

Once a network with the desired properties has been generated, ADHL can be simulated according to the model to be described in the next section.

3. Adsorption–Desorption Process

3.1. Theoretical Background. Basically, the method employs the well-known Broekhoff and de Boer equation,²⁹ which is a generalization of the classical Kelvin equation for condensation–evaporation processes on curved liquid–vapor interfaces

$$RT \ln \frac{p_0}{p} = F(t_c) + \frac{\gamma v}{R_m} \quad (9)$$

where $RT \ln(p_0/p)$ is the so-called *adsorption potential* or *differential adsorption work*.³⁰ It could also be identified as the difference in the chemical potential between a saturated phase at an equilibrium liquid–vapor pressure p_0 and an adsorbed one at a pressure p , both at the same temperature T . This adsorption potential has two parts. The first, due to the presence of the solid surface and lateral interactions among the adsorbate molecules packed at a liquidlike density and forming an adsorbed layer of thickness t . This potential is only a function of t and is given by the so-called *universal t curve* relation:³⁰

$$F(t) = 2.303RT \left[\frac{16.11}{t^2} - 0.1682 \exp(-0.1137t) \right] \quad (10)$$

For a curved adsorbed layer with local thickness t_c , t must be replaced by t_c in this equation. This takes into account the correction to the differential adsorption work due to the surface curvature.

The second part of the potential is due to the meniscus separating the adsorbed phase from the vapor phase, $\gamma v/R_m$, where γ and v are the adsorbate surface tension and molar volume, respectively, and R_m is the mean curvature radius of the interface. Moreover, γ varies with the mean curvature radius as $\gamma_0 R_m/(R_m - \sigma)$,³² where γ_0 is the surface

tension for a plane layer and σ is the effective molecular diameter for the adsorbate. R_m is given by

$$\frac{1}{R_m} = \frac{1}{R_1} + \frac{1}{R_2} \quad (11)$$

where R_1 and R_2 are the principal curvature radii of the interface. Thus, for spherical and cylindrical pore geometry, the potential in eq 9 is given, respectively, by

$$RT \ln \frac{p_0}{p} = 2.303RT \left[\frac{16.11}{t_c^2} - 0.1682 \exp(-0.1137t_c) \right] + \frac{\gamma_0 v}{\frac{R_S - t_c}{2} - \sigma} \quad (12a)$$

$$RT \ln \frac{p_0}{p} = 2.303RT \left[\frac{16.11}{t_c^2} - 0.1682 \exp(-0.1137t_c) \right] + \frac{\gamma_0 v}{R_B - t_c - \sigma} \quad (12b)$$

In our network we assume that sites are spherical, and then represented by eq 12a, and that bonds are cylindrical, and then represented by eq 12b.

When adsorption takes place, the whole network is accessible to the gas. As pressure increases, t_c increases and its value can be found as a solution of these equations as long as the meniscus radius is above the Kelvin critical radius for capillary condensation. Therefore, a pore (site or bond) with an already adsorbed layer of thickness t_c at the previous pressure step will condense (not condense) at the new p_0/p value, if eq 12 does not have (has) a solution with a new t_c value (the absence of a value of t_c satisfying the equation means that capillary condensation already occurred). In the case of the condensation in sites, an additional condition to ensure vapor meniscus continuity, i.e., that at least $Z - 1$ of the connected bonds (Z being the local network connectivity) must be previously filled with liquid, must also be fulfilled for condensation to occur.³³ This last condition, ensuring continuity in the liquid–vapor interface, is, however, not always considered in the literature, and we will also explore the consequences of dropping it.

For the desorption stage, a pore (site or bond) will evaporate at a p_0/p value if its hemispheric curvature radius R_m is greater than the critical Kelvin radius, $R_K = \gamma_0 v/RT \ln(p/p_0)$, corresponding to that pressure, and if, in addition, such a pore is *connected to the vapor phase by a continuous path of already evaporated pores*. This last condition introduces cooperative effects in the desorption branch which can be expressed by the relation⁸

$$[1 - V_{\text{des}}(R_K)] = [1 - V_{\text{ad}}(R_K)] P_B(Z_q) \quad (13)$$

where V_{ad} (V_{des}) is the volume filled with adsorbate in the adsorption (desorption) branch, q is the fraction of bonds with $R > R_K$ (both Z and q calculated for those sites with

(24) Mayagoitia, V.; Cruz, M. J.; Rojas, F. *J. Chem. Soc., Faraday Trans 1* **1989**, *85*, 2071.

(25) Riccardo, J. L.; Steele, W. A.; Ramirez, A. J.; Zgrablich, G. *Langmuir* **1997**, *13*, 1064.

(26) Riccardo, J. L.; Pereyra, V.; Zgrablich, G.; Rojas, F.; Mayagoitia, V.; Kornhauser, I. *Langmuir* **1993**, *9*, 2731.

(27) Adrover, A.; Giona, M.; Giustiniani, M. *Langmuir* **1996**, *12*, 4272.

(28) Adrover, A. *Langmuir* **1999**, *15*, 5961.

(29) Broekhoff, J. C. P.; de Boer, J. H. *J. Catal.* **1967**, *9*, 8.

(30) Dubinin, M. M. *Chem. Rev.* **1960**, *60*, 235.

(31) Lipkens, B. C.; Linsen, B. G.; de Boer, J. H. *J. Catal.* **1964**, *3*, 32.

(32) Defay, R.; Prigogine, I.; Bellemans, A.; Everett, D. H. *Surface Tension and Adsorption*; Longmans: London, 1966.

(33) Mayagoitia, V. *Catal. Lett.* **1993**, *22*, 93 and references therein.

$R > R_K$), and P_B is the percolation probability for the bond problem. This percolation factor produces an inhibiting effect during the evaporation process: the larger the percolation threshold, the greater will be the retarding on the evaporation branch.⁸

Once a pore fulfills the two desorption conditions at a given p_0/p , it is evaporated leaving a liquid layer of thickness t_c , where t_c is again the solution of eqs 12a and b for spherical and cylindrical cavities, respectively, at that relative pressure. Each time p_0/p decreases, t_c is recalculated by means of eq 12 for each partially filled pore until it empties completely.

3.2. Simulation Algorithm. Cubic porous networks of $L \times L \times L$ are generated sampling the site and bond radii from given distributions with the same shape, the bond distribution being shifted to lower radii. We consider two kinds of distributions: the Gaussian and the Gamma distribution.

(i) Gaussian Distribution. We used two truncated and renormalized Gaussian distributions, with mean values S_m and B_m for sites and bonds, respectively, and the same standard deviation σ . The limits for sampling radii for sites and bonds were chosen to be $S_m \pm 2\sigma$ and $B_m \pm 2\sigma$, respectively.

(ii) Gamma Distribution. We used two truncated and renormalized Gamma distributions of the form $\Gamma(R) = (R - R_0)^{n-1} e^{-(R - R_0)}$, truncated at the upper limit at the value $R_0 + 2n$. The values of site and bond radii at maximum probability (S_m and B_m , respectively) are obtained in each case as $R_0 + (n - 1)$.

Samples with different overlapping, and then with different correlation length, were generated by moving the bond distribution to the right while keeping the site distribution fixed. Once the desired porous network is generated for a given kind of distribution by following the method described in section 2, sorption isotherms are simulated, recording the adsorbed or desorbed volume V as a function of p_0/p .

Starting at $V = 0$, the adsorption branch algorithm employed was as follows:

- A p/p_0 value is fixed.
- t_c is calculated for each bond connected to a site i, j, k by using eq 12b,

if eq 12b has solution *then* the adsorbed layer on that bond is actualized.

else, that bond condenses.

V does not change in any case because no volume is associated to bonds.

- t_c for site i, j, k is calculated using eq 12a,
- if* eq 6a has a solution, *then* the adsorbed layer on the site is actualized and V is actualized.

if eq 12a has no solution *and* the number of its filled connected bonds is $\geq Z - 1$, *then* that site condenses and V is actualized.

- i, j, k is looped until the entire network is inspected.
- The relative pressure value is increased and all the above repeated until $p_0/p = 1$.

Starting at $V = 1$, the desorption branch algorithm employed was as follows:

- A p/p_0 value is fixed (starting from 1).
- A number of bonds at the external faces of the cube are connected to the gas phase. t_c is calculated for each of them using eq 12b,

if eq 12b has solution, *then if* $R_m = (R_B - t_c)/2 \geq R_K$ the bond evaporates leaving a layer of thickness t_c .

- Elements (sites and bonds) in the whole network are inspected,

if the element is connected to the gas phase, *then* t_c is calculated.

Table 1. Overlapping Values for Different σ and d

σ	d	Ω
1	10	0
5	10	0.3
10	10	0.6
10	35	0.04

If it is a site and eq 12a has solution, *then* it is evaporated leaving a layer of thickness t_c and V is actualized.

If it is a bond, the procedure is the same as for surface bonds.

- The relative pressure value is decreased and all the above repeated until $p_0/p = 0$.

4. The Behavior of Adsorption–Desorption Hysteresis Loops

Actual calculations were carried out by assuming N_2 at 77 K as the adsorbate. To eliminate spurious effects in the desorption branch due to a high surface-to-volume relation in a cubic network of size $L \times L \times L$ (with L moderately small), it was necessary to connect the sample to the vapor phase through just one single bond on the external faces of the cube. Moreover, it was determined that finite size effects became negligible for $L = 50$, so that this was the size finally used to obtain our results.

A first series of ADHL was obtained for site and bond Gaussian distributions with σ ranging from 1 to 20, S_m from 75 to 240, and $d = S_m - B_m$ from 10 to 75 (all size and distance units are in angstroms). The overlapping Ω , and then the correlation length l_0 , depends on both σ and d . As an example, a few values are given in Table 1.

In Figure 1, the behavior of ADHL as S_m changes, when σ and d are fixed, can be observed. The different Gaussian site and bond distributions used are shown in the inset. The adsorption branch, and consequently the whole ADHL, moves to higher relative pressure as S_m increases, as expected. The partial saturation shoulder on the adsorption branch is readily explained due to the cooperative effect introduced by the condition that $Z - 1$ connected bonds must condense before a site is allowed to condense. In fact, when bond and site distributions are close enough as in this case, spatial correlation is strong and a large site is probably surrounded by large bonds, thus retarding more the condensation process (it should also be considered that bonds have a cylindrical geometry, thus doubling the mean curvature radius). On the contrary, when the distributions are far apart, the correlation length is nearly zero and a large site is probably surrounded by several smaller bonds, which have already condensed, and the retarding effect on condensation should become much smaller (as will be shown below). The desorption branch presents a well-defined knee, whose position should be in close correspondence with the percolation threshold, according to eq 13. As we can see, the ADHL is wider, and the percolation threshold higher, when pore sizes are generally smaller (lower values of S_m), even though the overlapping Ω between site and bond distributions remains the same. However, due to the retarding effect on the adsorption branch just discussed above, the variation in the wideness of the ADHL cannot be attributed entirely to the bond percolation threshold.

Figure 2 shows the behavior of ADHL for fixed S_m and σ as d changes. As discussed above, the shoulder in the adsorption branch gradually disappears as d increases and consequently the correlation length decreases. We now observe that the position of the knee in the desorption branch shifts to lower pressure as d increases; however at the same time the wideness of the ADHL also decreases. The first effect was to be expected from two-dimensional

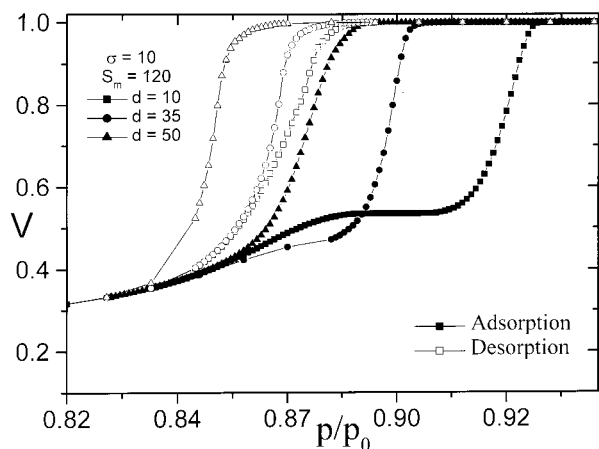


Figure 2. ADHL for Gaussian site and bond distributions for fixed σ and S_m showing the effect of the shift in the bond distribution, d .

results,¹⁵ where it was found that the bond percolation threshold increased as the overlapping between site and bond distributions (and then the correlation length) decreased. The second one is the consequence of the disappearance of the cooperative effect on the adsorption branch as d increases.

From the above it turns out that the position of the desorption knee, which we denote as p^* , should be a relevant parameter to describe the behavior of ADHL since it reflects directly the percolation properties of the porous network independently of the way in which condensation took place. Of course, the exact value of this parameter depends on the way in which this relative pressure is determined from the desorption branch, and this could be quite arbitrary. Just to fix a simple criterion, we take as p^* the value of the relative pressure where the normalized adsorbed volume takes the value 0.9 on the desorption branch. With this we obtain the variation of p^* as a function of d , for different values of S_m and σ , shown in Figure 3a. As we can see, we have different families of curves for each value of S_m , and in each family p^* decreases with d , the decrease becomes quicker as the value of σ becomes smaller.

We now want to study the effects of changing the shape of site and bond distributions, by using the Gamma distribution, and also the effects of dropping the condition that $Z - 1$ bonds should have condensed in order that the connected site can condense if it has reached the Kelvin radius. Under these conditions we obtain the ADHL shown in Figure 4. The three series, from top to bottom, are obtained with the same value of $n = 5$, and each one corresponds to a given S_m . Within each series the different loops are for different values of $d = S_m - B_m$. We observe, as expected, that we do not have any cooperative effect in the adsorption branch, which is the same for each series, and that the desorption knee shifts to lower pressure as d increases, indicating an increase in the percolation threshold. The behavior of p^* as a function of d , for different values of S_m and n , shown in Figure 3b, is similar to that obtained in the case of the Gaussian distribution.

In what follows we intend to use the observed behavior of ADHL in proposing a characterization method, overcoming limitations of classical methods.

5. Characterization Method

Classical characterization methods to obtain site and bond distributions from experimental ADHL have been extensively discussed in refs 1 and 6. All methods are

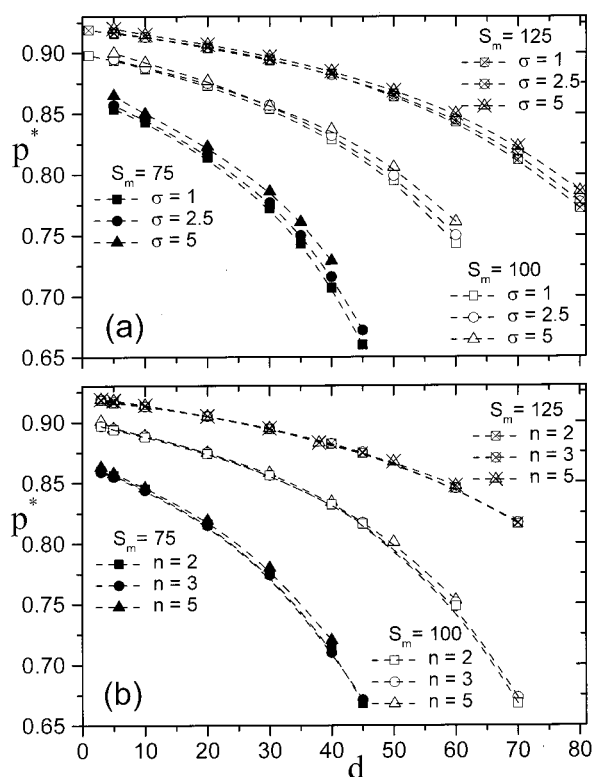


Figure 3. Variation of the desorption knee relative pressure, p^* , with the shift between site and bond distributions: (a) Gaussian distribution; (b) Gamma distribution.

similar, in the sense that they are developed under the assumption that no spatial pore size correlations are present in the network. To test the validity of the predictions of these methods against the simulation results obtained above for a given ideal porous network, we shall use them in predicting the bond distribution, given the site distribution, from simulated ADHL.

In particular, we consider the method described in ref 6 for the same ideal porous network considered in our simulations, i.e., spherical sites and cylindrical bonds, the adsorbed volume in bonds being negligible. According to this method, the hysteresis loop is described by eq 13, where, neglecting correlations, the relation between the parameter Zq and the Kelvin radius R_K is given by

$$Z_q = Z_0[1 - B(R_K)]/[1 - S(R_K)] \quad (14)$$

where S and B are the integral site and bond distributions defined by eq 1. In addition, the method makes use, in eq 13, of the “universal” bond percolation probability due to Kirkpatrick,³⁴ valid for three-dimensional uncorrelated networks:

$$P^B(x) = \begin{cases} 0; & x < 1.5 \\ 1.54(x - 1.5)^{0.4}/[1 + 0.606(x - 1.5)^{0.4}]; & 1.5 \leq x \leq 2.7 \\ 1; & x > 2.7 \end{cases} \quad (15)$$

Now the method proceeds as follows: given the site distribution, $F_S(R)$, and the simulated “experimental” ADHL, $P^B(Zq)$ is obtained using eq 13 and then Zq is obtained by inverting eq 15. With this, $B(R_K)$ is calculated from eq 14 and, finally, $F_B(R)$ is obtained by differentiation.

(34) Kirkpatrick, S. *Rev. Mod. Phys.* **1973**, *45*, 574.

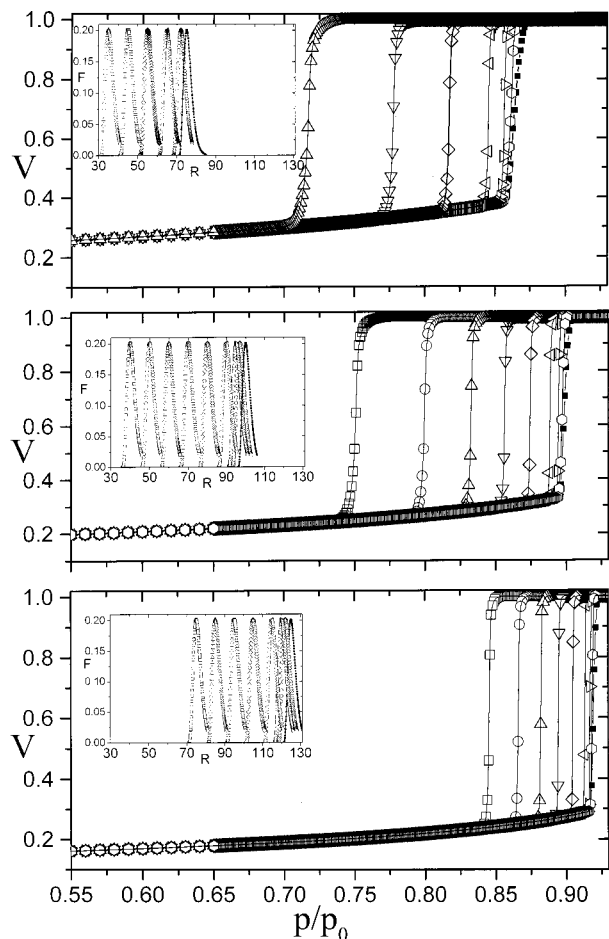


Figure 4. ADHL for Gamma site and bond distributions. The inset shows the site (full squares) and bond (open symbols) distributions used in each case.

Figure 5 shows the test of this method for the case of the Gaussian distribution with $S_m = 100$ and $\sigma = 5$, for different values of d . In each case the full line represents the given site distribution, the broken line the actual theoretical bond distribution, and the open circles (with line to guide the eye) the bond distribution predicted by the above classical method. Important deviations are evident, especially in the case of important overlapping between actual site and bond distributions (upper part), corresponding to stronger spatial correlations.

From these results we infer that classical characterization methods not taking into account spatial correlations (i.e., they force the medium to be completely random) have serious limitations and that new methods are necessary.

Our analysis of the effects of percolation on ADHL for correlated networks suggests that the position of the bond distribution, determined by B_m , and the relative pressure at the desorption knee, p^* , are the two most relevant parameters. When all results for the Gaussian and Gamma distributions, represented in Figure 3, are cast together in a graph of B_m as a function of p^* , Figure 6, we see that all the data come on a single “quasi-universal” curve, given, by means of a least-squares curve fitting, by the simple equation

$$B_m(\text{nm}) = \frac{1}{1 - p^*} \quad (16)$$

where B_m should be measured in nanometers. This is a quasi-universal equation in the sense that, at least for the variations we have considered here, it does not depend

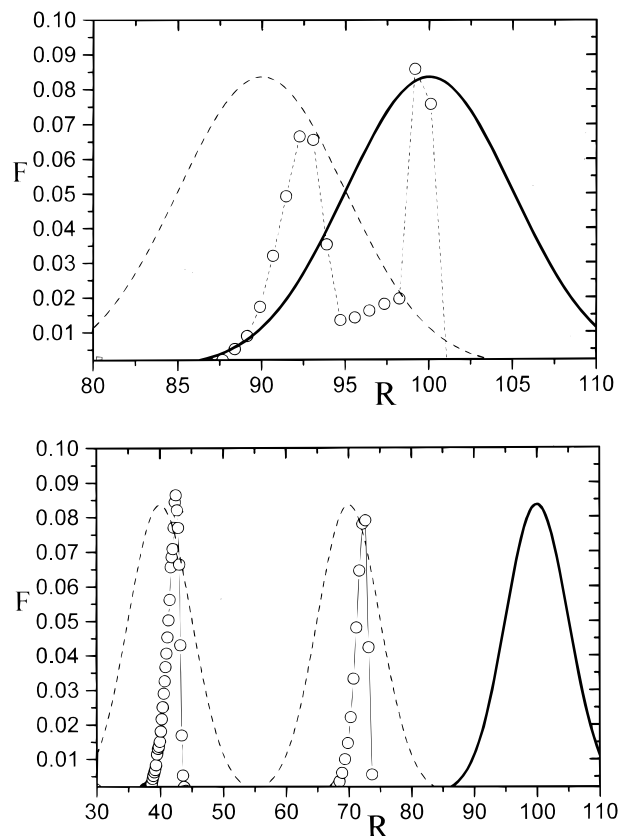


Figure 5. Numerical test for classical characterization methods: the thick full curve represents the site distribution used, the dashed curve represents the bond distribution used, and the open circles are the predictions of the method given in ref 6.

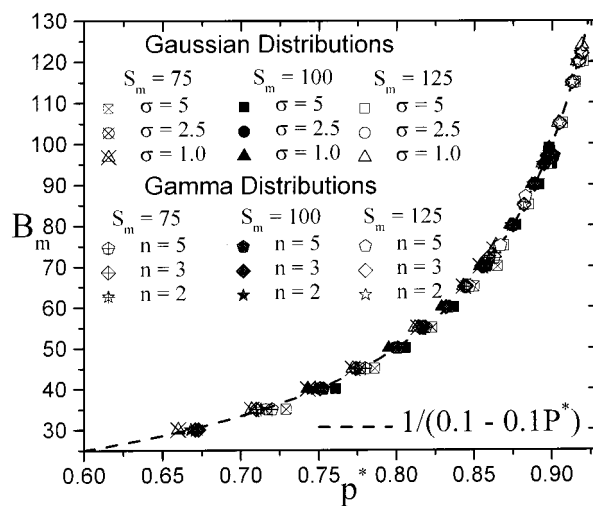


Figure 6. Quasi-universal empirical relation between B_m and p^* showing the collapse of all the data corresponding to Figure 3 on a single curve.

on the shape of the size distribution and its mean square deviation, or on the position of the site distribution, or even on the adsorption process considered (cooperative effects from $Z - 1$ bonds for the condensation in a site). The universality is limited by the facts that we considered a network whose pore volume is essentially attributed to the sites and that we considered the weakest possible form of correlation, i.e., the one imposed by the construction principle and given by the dual site–bond model. At the present time we do not have a theoretical or approximate scaling justification of this equation, and it should be taken

as an empirical law. A better understanding of how this relation arises could be achieved through the study of percolation probabilities in three-dimensional correlated networks, not available at the moment.

Equation 16 can now be used to propose a characterization method, which we believe is a first realistic approach to obtain the site and bond size distributions from experimental ADHL of vapors for mesoporous materials. The method can be described through the following steps:

(i) Obtain the size distribution for sites from the experimental adsorption branch. This, assuming that the volume associated with bonds is negligible, can be easily achieved from a differential analysis of that branch.^{1,2}

(ii) Independently of the shape of the distribution obtained for the sites, assume the same shape for the bond distribution. This is not a too strong restriction, considering that other quite stronger restrictions are necessarily made in any method, like the one regarding the pore geometry (sites and bonds).

(iii) Obtain p^* from the experimental desorption branch and calculate B_m from eq 16. This will give the positioning of the bond distribution.

6. Conclusions

We have studied through Monte Carlo simulation how ADHL are affected by the topological characteristics, closely related to the percolation characteristics, of correlated three-dimensional porous networks described by the DSBM for Gaussian and Gamma size distributions. We have in addition assumed that the pore volume in our networks resides mainly in the sites, whereas bonds only contribute to percolation effects. The use of the DSBM has the advantage that once the shape of site and bond size distributions is fixed, the topological characteristics of the porous network depend on a single parameter, the overlapping Ω between those distributions (closely related to the correlation length of the network, eq 8).

A wide range of the parameters has been investigated, and we have found out that all results can be conveniently represented in terms of two main variables: p^* , the relative pressure at the desorption knee in the ADHL,

and B_m , the size of maximum probability in the bond distribution. By use of these two variables, all results scatter closely around a characteristic quasi-universal curve, eq 16. These findings provide us with a method to determine the site and bond distributions for correlated networks from the analysis of experimental ADHL.

The proposed method represents a first realistic approximation to the solution of the characterization problem for mesoporous materials, given that (a) realistic mesoporous disordered material cannot be completely random and present spatial correlations in pore sizes, (b) classical methods based on random networks show important deviations in the determination of the bond distribution, given the site distribution, (c) the DSBM is the simplest available model to describe a porous network with the minimum degree of correlation, namely, that imposed by the construction principle, (d) the desorption branch of the ADHL is mainly determined by the bond percolation probability, however this has only been obtained in the framework of the DSBM for Cayley trees (no closed loops) and for two-dimensional networks, and (e) the proposed method overcomes the deviations of classical methods in the sense that it is better to consider just the minimum degree of correlation, which should be common to all porous networks, than considering no correlation at all.

Our final conclusion is that a general and realistic characterization of mesoporous materials still remains as an open problem. Further developments should be directed to investigate the percolation probabilities in three-dimensional porous networks, described, in a first step, by the correlations considered in the DSBM, and then networks with stronger correlations. The effects of the network topology in a model where the main porous volume is attributed to the bonds (the opposite of the present model) should also be investigated, to end up finally with the general case where the porous volume is shared by sites and bonds.

Acknowledgment. This research was partially supported by the Consejo Nacional de Investigaciones Científicas y Técnicas (CONICET) of Argentina.

LA991465+